

Enhancements Toward Robust Normal Point Generation

John H. Seago

AlliedSignal Technical Services Corporation
7515 Mission Drive, Lanham, MD, 20602 USA

Abstract

This paper describes fundamental changes to a contemporary version of the NASA Satellite Laser Ranging Generic Normal Point Processor. The basis of this upgraded process is the former normal point generator with numerical improvements added to suppress sporadic deficiencies and bolster overall product quality. The new algorithm incorporates modern numerical treatments of the solution of least-squares normal equations, tangible criteria for gauging the optimality of trend functions, and the application of robust estimation theory toward initial outlier rejection. A simple median filter, in combination with other robust estimators, aids to identify the primary trends embedded in noisier data sets. The enhanced processor was validated by comparing normal point residuals against precise long-arc ephemerides under worse case scenarios. A public domain version of the software is anticipated.

A. Overview

1. Problem Summary

Recently, recurring anomalous SLR normal points were noted by analysts (R. Noomen, Personal Communication) in the SLR normal point product from stations using the on-site NASA Generic Normal Point Algorithm (known here as GNP-1). Such anomalies usually appear at the extremities of a pass when compared against *post facto* long-arc trajectory solutions (see Figure 1). Mild signal remaining in the residual track is another, but less well known, problem. This residual signal is often observed on long passes with high tracking densities, typical of LAGEOS tracking. Additionally, the NASA SLR Mission and Data Operations Group of AlliedSignal Technical Services Corporation (ATSC) manually reprocesses all NASA SLR full-rate observations of the GPS-35 and GPS-36 satellites. This effort is necessary due to the historically poor quality of the SLR normal points ranging to GPS altitudes. Many software enhancements were added to GNP-1 to diagnose abnormal normal points, culminating into a second-generation program referenced herein as GNP-2 (Figure 4). The scope of this upgrade has not yet encompassed alternative bias functions or trend function recommendations (see Appleby and Sinclair, 1992).

2. Overview of the GNP-1 Processor

The NASA Generic Normal Point Processor GNP-1 has grown out of the original Herstmonceux recommendations (Sinclair, 1997). The process was initially expanded to include a short arc state update to accommodate deteriorating predictions. The Poisson filtering technique developed at MLRS for LLR applications was later incorporated to facilitate daytime tracking (Ricklefs and Shelus, 1992, Jefferys and Ries, 1996). The GNP-1 algorithm also shares some of the SLR editing techniques employed by the University of Texas Center for Space Research (Davis et al., 1997, p. 455). However, the GNP-1 process typically estimates several more degrees of freedom since the dynamic orbit model is based on the so-called "tuned IRV". This dynamic model has certain deficiencies for very low or very high altitude satellite trajectories (Sinclair, 1994). Conklin et al. (1994) provides a detailed description.

The Herstmonceux algorithm is predicated on the availability of high precision predictions, best available *a priori* time bias, and possibly corrections to the predicted UT1 values. Applying these recommended corrections reduces the magnitude of the residuals so one can choose a suitable range window to remove the largest outliers. The GNP processes are exceptional because no mechanisms exist to supply these corrections. Residuals against a biased IRV prediction have been observed to approach one kilometer, encumbering initial outlier rejection.

GNP-1 prefers to estimate its own bias functions on a pass-by-pass basis (see Appleby and Sinclair, 1992), but the presence of substantial outliers can occasionally corrupt these *in situ* bias estimates. When noise levels are exceptional, editing is deferred to the Poisson filter. Poisson filter performance is optimal in the presence of a flat residual track, and gains may be possible with the tailoring of satellite-specific parameters originally adjusted via user interaction

(Ricklefs and Shelus, 1992). However, the GNP-1 implementation of the Gauss filter lacks this kind of fine tuning and sporadically retains measurement noise during unfavorable circumstances.

3. The Origin of Bad Normal Points in GNP-1

Investigation has confirmed that bad normal points are the manifestation of anomalous full-rate tracking data not initially culled from the full-rate measurements. Outlier rejection is aggravated by the fact that, for noisier passes, recursive editing with an RMS multiplier is less effective when noise inflates the RMS values. An unconstrained trend function (defined as a function of time) is also prone to consider any datum *isolated in time*, known as a "leverage point" (Wadsworth, 1989, p. 16.14). Once a time-isolated outlier, or bad leverage point, has corrupted the trend function, it cannot be removed with RMS multiplier editing. The inclusion of bad data in a weakly tracked pass has been known to corrupt the nominal estimation of the trend function across adjacent normal point windows. This is especially true at the extremities of sparsely tracked passes, where the tracking density is insufficient to constrain the boundaries of the trend function in the presence of bad leverage point,s. Enhancements have therefore focused on the use of robustness methods to reject these outliers autonomously.

B. Robustness Methods

4. The Concept of Robustness

Outlier rejection is often accomplished via *robust estimation*. A qualitative definition of robustness "signifies insensitivity to small deviations from the assumptions" (Huber, 1981, p. 1). "Small deviations" can imply either a small number of sizable deviations (outliers), or a sizable number of small deviations (abnormal distribution) (Press et al., 1992, p. 694). For example, statistical interpretation of a least-squares estimator presumes the errors are normally (Gaussian) distributed and without bias, yet SLR data are frequented with outliers where such distributional assumptions are violated. Numerous papers also acknowledge systematic biases and non-Gaussian densities due to satellite signature and detector characteristics (Sinclair (ed.), 1995), but the immediate emphasis is on the estimation of trends from noisy time series.

The use of robust estimators on SLR data is not novel: robustness is the primary concept driving the Herstmonceux algorithm. Regarding other work specific to SLR, Paunonen (1992) uses an "adaptive median filter" minimizing the median absolute error, and Detong et al. (1992) cites success with Hampel M-estimates.

5. M-Estimators

The reader is directed to the following references as a starting point for more comprehensive discussions of robust M-estimators: Press et al. (1992), Hogg (1977), Huber (1996), Rey (1983), Wadsworth (1989). The following treatment is provided merely to convey notation, and to illustrate how the original Herstmonceux recommendations form a quasi-robust M-estimator. According to Huber, the generalized form of an M-estimate or maximum-likelihood-type estimate that minimizes the scalar performance index $J(\mathbf{X}_0^*)$ is:

$$J(\mathbf{X}_0^*) = \sum_i \rho(\mathbf{X}_0^*, Y_i) = \sum_i \rho(y_i) = \min! \Rightarrow \left. \frac{\partial J(\mathbf{X}_0^*)}{\partial \mathbf{X}_0^*} \right|_{\hat{\mathbf{x}}_0} = \sum_i y_i \psi(y_i) \frac{\partial G(\mathbf{X}_0^*, t_i)}{\partial \mathbf{X}_0^*} = 0; \text{ where } \psi(y_i) = \frac{d\rho(y_i, \mathbf{X}_0^*)}{d\mathbf{X}_0^*}$$

where $\rho(y_i)$ is an even function of the observation residuals y_i . For the general least-squares (LS) problem, $\rho(y) = y^2/2$ and $\psi(y) = y$. The observation residual y_i is the difference between the observed and the computed observation, sometimes abbreviated [O-C] and defined as:

$$y_i = Y_i - G(\mathbf{X}_0^*, t_i), \quad i = 1 \rightarrow n \text{ (scalar); -or- } \mathbf{y} = \mathbf{Y} - \mathbf{G}(\mathbf{X}_0^*, t_i) \text{ (vector)}$$

where Y_i is an n vector of observations at times t_i , $G(\mathbf{X}_0^*, t_i)$ is an n vector containing the calculated value of the observations at times t_i based on state variables \mathbf{X}_0^* using a geometrical or physical observation/state relationship. The performance index is minimized by taking the partial derivative of an analytical expression for $J(\mathbf{X}_0^*)$ with respect to the estimated parameters. Press et al. (1992, p. 696) presents a compelling analogy demonstrating that $\psi(y_i)$ is functionally equivalent to an observation weight w_i in the weighted LS algorithm. This implies that the underlying Gaussian error distribution can be augmented to represent a more realistic distribution via the $\psi(y)$ function. For a continuous probability density function $f(y)$, the ordinary maximum likelihood estimator for that distribution will take the form $\rho(y) = -\ln|f(y)|$ (Huber, 1996, p. 13), or alternately $f(y) = e^{-\rho(y)}$. The ψ -function is the derivative of this $\rho(y)$.

Derivation of the so-called normal equations that minimize the LS performance index is adequately detailed in numerous texts (i.e., Vallado, 1997); again, this limited presentation merely defines notation. Given a vector of n observations \mathbf{Y} and a vector of m parameters \mathbf{X}_0^* to estimate, the normal equations that represent the *minimum variance estimate* (or *maximum likelihood estimate*) of the weighted LS problem are satisfied by the matrix-vector expression:

$$\hat{\mathbf{x}} = [\mathbf{H}^T \mathbf{W} \mathbf{H}]^{-1} [\mathbf{H}^T \mathbf{W} \mathbf{y}] ; \quad \mathbf{X}^{(k)} + \hat{\mathbf{x}}^{(k)} = \mathbf{X}^{(k+1)}$$

where \mathbf{H} is the $(m \times n)$ design matrix of partials, \mathbf{W} is an $(n \times n)$ weight matrix, \mathbf{y} is an $(n \times 1)$ residual vector such that:

$$\mathbf{H} = \frac{\partial \mathbf{G}(\mathbf{X}_0^*, t_i)}{\partial \mathbf{X}_0^*} ; \quad \mathbf{W} = \begin{bmatrix} w_1 & 0 & \text{L} & \text{L} & 0 \\ 0 & 0 & & & \text{M} \\ \text{M} & & w_i & & \text{M} \\ \text{M} & & & 0 & 0 \\ 0 & \text{L} & \text{L} & 0 & w_n \end{bmatrix} = \text{diag}(w_i) ; \quad \mathbf{y} = \mathbf{Y} - \mathbf{G}(\mathbf{X}_0^*, t_i) ; \quad i = 1 \rightarrow n$$

Huber was one of the first to describe an algorithm for robust single parameter M-estimates, cited as the ‘‘Modified Weights’’ approach. In later literature (Coleman et al., 1980, Holland and Welsch, 1977, Jefferys, 1990), this technique is better known as *iteratively reweighted least squares* (IRLS). IRLS is directly applicable to the ordinary weighted LS normal equations, where the elements of the diagonal weight matrix \mathbf{W} (previously defined as *a priori* measurement variance) are iteratively scaled ($k = 1 \rightarrow \infty$) according to:

$$MAD = \text{median}\left\{ \left| y_i - \text{median}\{y_i\} \right| \right\} ; \quad \Delta_i = \frac{y_i}{\sigma(MAD)} \Rightarrow w_i^{(k)} = \frac{\psi(\Delta_i)}{\Delta_i}$$

Unlike the Herstromceux recommendation, the median absolute deviation (*MAD*) substitutes for RMS as the preliminary scale estimate. The diagonal weights w_i on the k^{th} iteration are used to update the state via the normal equations. Adequate statistical accuracy is usually attained within $k < 10$ iterations (Huber, 1996, p. 39), and experience holds this true for all but the noisiest SLR passes.

The Herstromceux algorithm is a form of quasi-robust IRLS M-estimator, because neglecting observations whose residuals exceed some multiple of the scale estimate (RMS) is equivalent to iteratively reweighting the LS solution with $w_i = 1$ or 0. In fact, data screening in this way supposes that the underlying distribution is Gaussian with heavy tails added to accommodate outliers (Holland and Welsch, 1977). Dependence on RMS as the scale estimate is a potential stumbling block: the RMS can be largely effected by marginal data on the shoulders of the distribution, and iterating the scale estimate tends to affect convergence in unpredictable ways. GNP-2 therefore applies a robust scale estimate based on *MAD* that does not require iteration, and scaled so it conforms to the conventional notion of standard deviation (Rey, 1983, p. 127):

$$\sigma \approx 1.4826 * MAD$$

6. Choice of IRLS M-Estimate

Herstromceux recommended weights of zero and unity can be augmented with a weight profile having more desirable robustness characteristics. One necessary characteristic for a robust estimator is that its ψ -function should be bounded for all values of Δ (Huber, 1996, p. 14), and ideally, the derivative of the ψ -function should be monotonically decreasing (Hampel, 1985). To illustrate these concepts, a short example is contrived using an approximate distribution function already introduced in the SLR literature (see Sinclair, 1995b, p. 39). This ‘‘peak-finding’’ distribution $f(\Delta)$ approximates the shape of the Gaussian distribution with trimmed tails, whose ρ -function can be found according the prescription:

$$f(\Delta) = \frac{1 - 0.15275\Delta^2}{1 + 0.41964\Delta^2} \Rightarrow \rho(\Delta) = -\ln \left| \frac{1 - 0.15275\Delta^2}{1 + 0.41964\Delta^2} \right| ; \quad \Delta < c$$

for the tuning constant $c = 2.558$. Differentiating, the corresponding ψ -function and weighting profile for IRLS are:

$$\psi(\Delta) = 1.14478\Delta \left[\frac{1 + 0.41964\Delta^2}{1 - 0.15275\Delta^2} \right] ; \quad \Delta < c \Rightarrow w_i = 1.14478 \left[\frac{1 + 0.41964\Delta_i^2}{1 - 0.15275\Delta_i^2} \right] ; \quad \Delta < c$$

For values of $\Delta > c$, the “peak-finding” distribution is set to zero, and it is presumed that the influence and weight are also meant to be zero. As an estimator, the “peak-finding” distribution has one of the properties of robustness because the ψ -function is bounded for infinite Δ (for finding the peak, the function is made more robust by setting $c = 1$, see Sinclair, 1995b). Although this distribution approximates the standard normal distribution, its ψ -function is less robust than an LS estimator using the same tuning constant, since the weight profile increases with Δ .

The previous example attempted to illustrate how the ψ -function can serve as a heuristic for gauging robustness. Not surprisingly, estimators are classified by the behavior of $\psi(\Delta)$. If $\psi(\Delta) = 0$ for sufficiently large $|\Delta|$ (such as the Herstromceux recommendation), the ψ -function is classified as a *redescender*. If $\psi(\Delta) \rightarrow 0$ asymptotically as $|\Delta| \rightarrow \infty$, the ψ -function is sometimes said to be a *soft-redescender*, and other bounded profiles can be classified as *monotone* (Holland and Welsch, 1977). GNP-2 replicates some aspects of a mathematical software package described by Coleman et al. (1980) to perform IRLS using various robust estimators. This experience has resulted in the preferential use of the weight profile associated with the ρ -function “Fair” (Fair, 1974). This appealingly simple ρ -function is well regarded (Rey, 1983, p. 110; Jefferys, 1990; Jefferys et al., 1988), and has the desirable property of being differentially insensitive to estimated scale (Holland and Welsch, 1977). The Fair function has nice convergence properties because it is everywhere defined continuous over the first three derivatives (Rey, 1983, p. 116). The Fair function as used by GNP-2 is:

$$\rho(\Delta) = c^2 \left[\left| \frac{\Delta}{c} \right| - \ln \left(1 + \left| \frac{\Delta}{c} \right| \right) \right]; \quad \psi(\Delta) = \Delta \left[1 + \left| \frac{\Delta}{c} \right| \right]^{-1}; \quad w_i = \left[1 + \left| \frac{\Delta_i}{c} \right| \right]^{-1}$$

where the tuning constant $c = 1.3998$ for 95% asymptotic efficiency on the standard normal distribution.

Experiments with GNP-2 on SLR full-rate data suggest that a combination of a monotone weighting profile followed by moderate \times RMS editing is an appropriate estimation technique for reducing trend functions, provided leverage points are initially down-weighted. Experience has shown that redescenders can initially nullify valid observations and adversely impact convergence. This limitation is affirmed by Hampel (1985, pg. 152) for iterative algorithms like IRLS.

C. GNP Enhancements

8. Weighting Scheme

In accordance with the Herstromceux recommendations, GNP-1 maintains a corresponding weight for every observation. The weights are either unity or zero depending upon whether the observations are deemed “valid” or “noise”, respectively. The drawback to this method is that an individual observation has either full influence or none: there is no way to slowly introduce suspicious or marginal data. GNP-2 introduces the variably weighted LS approach with valid weights ranging from zero to unity, according an alternate robust distribution (i.e., Fair). Suspected outliers and noise are suppressed for estimation purposes using the designator $w_i = -1$. Suspect data are ignored until they qualify under some future criterion (i.e., within \times RMS of some trend). If a negatively weighted value is ever to be reinstated, w_i is set to zero so it does not have undue initial influence.

9. Leverage Point Pre-Filter

Experience has dictated that, when the relative data density drops to a very low rate (less than one measurement per minute), it is highly plausible that the “time-isolated” measurements are no longer valid SLR observations. This is not unexpected since periods of lost target acquisition would result in the recording of noise only. Such sparse data are always highly prone to being accepted because they are leveraged. To suppress the formation of time-isolated outliers into bad single-point normal points, GNP-2 implements a *leverage point pre-filter* that initially flags heavily leveraged points as noise. Here, a datum is considered leveraged if it is the lone observation within a specified time period labeled the “isolation window”. The isolation window is arbitrarily chosen to be equal to either the recommended integration step size for the IRV integrator, or twice the normal point bin size (whichever is larger). These values are passed via a satellite data file containing other satellite specific parameters. The isolation windows for several satellites are listed in Table 1.

The leverage pre-filter is an important factor toward eliminating bad normal points, but its use comes with mild risk. It is unlikely, but still possible, to have high quality data consisting of nothing but highly leveraged points. All

leverage points are reconsidered later in processing once data trends have initially been assessed by higher confidence data. Their reintroduction may not be totally successful when the tracking is so sparse that the trends cannot be extrapolated unerringly, or the noise level exceeds 50% in that part of the pass.

10. Median Pre-Filter

GNP-2 introduces a *median pre-filter* to identify local trends in dense but noisy data. The median pre-filter first estimates an average based on a local sequence of N_{point} residuals, then compares this local average with the central value of the sequence. An initial weight is assessed based on the distance of the actual residual from the group estimate. The median pre-filter uses the median as its estimate of location (L-estimate) and arbitrarily chooses the initial weighting:

$$w_i = \max\left(0, \left(1 - \sqrt{|\text{obs}_i - \text{median}_i| / \text{MAD}_i}\right)^2\right)$$

where median_i is the median value of a window of N_{point} residuals, obs_i is the residual at time t_i , and MAD_i is the median absolute deviation of the N_{point} residuals. If the local MAD_i is very large relative to expected SLR observation scatter or the pass average, it indicates that no confidence can be placed in the local L-estimate. If the residual track is relatively flat across the entire pass (indicating no recognizable local trend), the working assumptions are violated and the filter is bypassed. The median pre-filter works optimally in the presence of steep residual gradients, regions where Poisson filtering is thought to be less effective (Ricklefs and Shelus, 1992).

A disadvantage to this filtering scheme is that it tends to unfairly fault $N_{\text{point}}/2$ points on the extremities of large data outages. This is one incentive for keeping the window size small. Another disadvantage is that the local trend can vary over a large window in a way that cannot be observed by a simple L-estimate. Studies by Andrews et al. (1972) also indicate that L-estimates with noise are less reliable when using a window size of $N_{\text{point}} < 10$ observations. GNP-2 uses a nominal window value of $N_{\text{point}} = 11$, (but also utilizes windows of 5 and 7 after the data have been pre-filtered). Experience dictates that larger window sizes provide more aggressive editing and are not recommended.

The previously discussed combination of initial weight function, median L-estimate, and small window sizes will nominally reject up to 50% of the residuals for densely tracked passes, with less aggressive data flagging when the tracking density falls. While this rejection rate appears excessive, the only purpose of the median pre-filter is to identify the local trend based on surrounding data. The best residuals selected by this filter are heavily weighted as a starting point for further trend reduction. Although crude, this filter can be quite effective on identifying the true signal embedded in very noisy passes having strong biases (Figure 2).

11. Short Arc Differential Correction

Observational residuals are partly minimized with a short-arc differential correction (DC) that updates the six element satellite state vector using the IRV satellite dynamics. Observations consist of reduced one-way ranges plus a tropospheric delay correction. Except for an elevation dependent empirical TOPEX correction, there is no attempt account for any satellite- or station-specific attributes within the software itself.

The stability and accuracy of the DC are improved in GNP-2 by reformulating the normal equations solution approach. GNP-1 solves the normal equations by first forming $\mathbf{H}^T\mathbf{W}\mathbf{H}$, and inverting a 6x6 system using Gaussian elimination with partial pivoting. Although computationally convenient, this practice results in significant information loss (see Golub and Van Loan, 1989, p. 225; Watkins, 1991, p. 187). Without *a priori* covariance, GNP-1 prevents such a linear system from becoming numerically singular by forcing operations involving \mathbf{H} into extended precision. GNP-2 solves the normal equations using Singular Value Decomposition (SVD) working on $\mathbf{W}^*\mathbf{H}$ (Press et al. 1992, p. 59). SVD adds computational expense, but it is justified since it best satisfies the definition of qualitative robustness described earlier. The GNP algorithm estimates parameters assumed to be observable (which may not be), and SVD is the best prospect in providing solutions to nearly singular systems. SVD is a recommended procedure for IRLS algorithms, since the system of equations can approach rank deficiency while iterating (Coleman et al., 1980, p. 330).

The derivatives that comprise the individual elements of the design matrix \mathbf{H} are finite difference numerical approximations. The differences are based on a numerical integration of the IRV dynamic model using perturbed initial conditions (Escobar, 1976, p.326; Vallado, 1997, p.687). The six finite differences used by GNP-1 take the form:

$$\frac{\delta\rho(\mathbf{X}_0)}{\delta\mathbf{x}_0} = \frac{\rho(\mathbf{X}_0 + \mathbf{x}_0) - \rho(\mathbf{X}_0)}{\mathbf{x}_0} - \left\{ \frac{1}{2} \mathbf{x}_0^2 \frac{\delta^2 \rho(\mathbf{X}_0)}{\delta\mathbf{x}_0^2} \right\}$$

where ρ is the computed slant range, \mathbf{X}_0 is the initial satellite state at the start of the pass, \mathbf{x}_0 is a small perturbation to the initial state, and the term in brackets is the first high order term neglected in the approximation (the neglected term is easily inferred via Taylor series expansion). The precision of this numerical approximation is often dependent on the optimality of \mathbf{x}_0 , but assessing its adequacy proves difficult without corresponding analytical formulations. Experience with the GNP processes has shown that the perturbation \mathbf{x}_0 must be minuscule to be consistently effective, on the order $10^{-10}\%$ of the modulus of the position or velocity vector. This contradicts the cited literature, which typically recommends values of a few percentages (admittedly, the same literature does not particularly advocate the use of finite differences due to its imprecise nature). The GNP algorithms find usable values for \mathbf{x}_0 by first initializing these perturbations as insignificant but non-zero numbers. These are incremented until $\rho(\mathbf{X}_0 + \mathbf{x}_0) - \rho(\mathbf{X}_0)$ exceeds a significant level of the floating point accuracy (Press et al., 1992, p. 883). Evaluated this way, finite differences can be overwhelmed by numerical error because they represent the difference of two large numbers divided by a very small number. Steps were introduced in GNP-2 to ensure that \mathbf{x}_0 is always a number that has an exact binary representation (Press et al., 1992, p. 181), which preserves accuracy otherwise lost by division.

A *central differencing* equation is introduced for derivative approximation in GNP-2 (Vallado, 1997, p. 687):

$$\frac{\delta\rho(\mathbf{X}_0)}{\delta\mathbf{x}_0} = \frac{\rho(\mathbf{X}_0 + \mathbf{x}_0) - \rho(\mathbf{X}_0 - \mathbf{x}_0)}{2\mathbf{x}_0} - \left\{ \frac{1}{3} \mathbf{x}_0^3 \frac{\delta^3 \rho(\mathbf{X}_0)}{\delta\mathbf{x}_0^3} \right\}$$

where the term in brackets is again the first high order term neglected. This difference equation is twice as expensive to evaluate since it requires two evaluations based on both positive and negative deviations of the nominal initial conditions. A very small initial perturbation \mathbf{x}_0 still seems to be required, but this form is more qualitatively robust (because a central difference more closely approximates an analytical derivative).

The GNP-1 DC estimator employs the standard unweighted least squares with \times RMS editing, while GNP-2 uses a more robust ‘‘Fair’’ estimator initially. GNP-2 also attempts a goodness-of-fit test (Press et al., 1992, p. 657) to evaluate whether robust estimation is warranted; if not, a faster \times RMS editing scheme is adopted.

12. Selective Sampling

The computationally intensive GNP processes attempt to work with subsets of the total data to reduce CPU load. Sampling in GNP-1 was a simple process that chose every N^{th} point based on the amount of reserved memory. For example, GNP-1 limits the numerically rigorous DC process sample size to 120 observations: for a pass containing 1000 SLR measurements, every 8th observation is considered for the state update. Unfortunately, this kind of sampling does not explicitly account for the variable observation densities encountered during the pass. GNP-2 introduces the notion of *selective sampling* which chooses samples based on the pre-filter weights and tracking density. When tracking becomes sparse, data are preferred based on their time distribution, while data over densely observed regions are preferred based on the quality of pre-filter weights. GNP-2 is currently configured to use up to 500 pre-qualified, selectively sampled observations in the state update. Because sampling can be scaled via a single FORTRAN parameter, SVD is not necessarily a computational bottleneck on slower machines.

13. Bias Function

After the state update, a pass-specific bias function is estimated and removed. The function has three terms: a range bias P , a timing bias T , and a higher order unit-less term called the force-model bias Γ . This function takes the form:

$$B(t_i) = P_{bias} + \dot{\rho}_i T_{bias} + \dot{\rho}_i t_i \Gamma_{bias}$$

GNP-1 estimates the coefficients of this function by solving the normal equations using Cramer's rule with $3\times$ RMS editing. GNP-2 has maintained the same functional relation, but estimates these coefficients using SVD and IRLS. This change is necessary since GNP-1 may not recognize when the time-bias coefficient is approaching unobservability, which occurs when the satellite is only tracked briefly near the point of closest approach. The maximum allowable condition number is chosen to be $\kappa(\mathbf{H}) = 10^8$, which is small relative to the capabilities of double precision arithmetic. The estimated time bias

is applied to the IRV epoch early in the GNP-2 process, prior to attempting a differential correction. The complete bias function is estimated and applied after the differential correction update (Figure 4).

14. Sliding Polynomial Edit

GNP-2 introduces a “sliding polynomial edit” that successively estimates 3rd order polynomials over a sliding window of residuals. The polynomial residuals are used to re-weight the SLR observations after the satellite state update. This editing is necessary because the state update and bias function estimates are based on samples, and the observation weights for the rest of the SLR data trend are no longer consistent with the sample set weights returned from the DC. By re-initializing the weights in this way, the final trend function evaluation will usually converge faster.

15. Final Trend Function Evaluation

The GNP-1 process uses a variable order polynomial as a function of time to model remaining trends in the residual track. Appleby and Sinclair (1992) suggest a bias function in terms of RTN space (radial, transverse, normal) as a natural basis for removing orbit error. However, GNP-2 still maintains a time-varying polynomial trend at this time.

In all cases, GNP-1 uses a generic Nth order time polynomial as the basis for the final trend, but there are subtle defects in the logic that selects the optimal polynomial (Figure 1). In practice, the polynomial order is successively increased until the RMS fit does not change much, and the final polynomial evaluated is assumed the best fit. As designed, the polynomial is slightly over-estimated because the RMS was substantially reduced using the *previous* iteration, not the final one. A more serious problem occurs because convergence is assumed when one additional degree of freedom does not improve the RMS fit. In many cases, two low-order polynomials might have equally poor fits (showing no improvement in RMS), and the process stops prematurely. This is a primary source of residual signature found in long, high density passes.

GNP-2 evaluates several degrees of polynomials using Chebyshev basis functions, then compares results to choose the most effective polynomial. Minimum RMS is not always a good indicator of the best trend function because any arbitrarily high order function can accommodate existing noise and claim the smallest RMS. Instead, certain polynomial attributes are reduced to numbers, then weighted and summed to give each polynomial its own relative “score”. The polynomial that ranks highest is chosen as the optimal trend function, and in the unlikely event that multiple functions receive the same score, the least-complicated polynomial is selected. For example, minimum RMS fit is heavily weighted in the scoring because it is considered an important attribute, but other attributes consider the shape of the remaining residual signal, the amount of data rejected on the extremities of a pass, the quantity of single-point normal points, and total number of rejected normal points for each polynomial. A more complicated matter is determining the relative weights between these attributes, which has been investigated only to the point that the software is autonomously functional, but not necessarily optimal.

16. Other Features

The GNP-2 source code is considerate of FORTRAN 77 standards to facilitate cross-platform compatibility. Statements longer than 72 characters, extended precision (REAL*16) variables, antiquated FORTRAN IV constructs, and non-standard characters present in GNP-1 were eliminated. GNP-2 also adds over 700 meaningful comment statements, and most subroutines are now well documented. Place holders exist for alternate robust weight functions, and extensive debugging features can be activated by the user, including the capability to graph data at various stages of preprocessing.

D. GNP-2 Validation

17. Normal Point Validation

Although this paper emphasizes the theory and operational improvements to the GNP normal point process, a cursory assessment of the performance of the GNP-2 product is also warranted. GNP-2 normal points are validated by comparing the GNP-2 normal point product to a long arc SLR solution based on GNP-1 normal points, and by comparison against the GNP-1 normal points themselves. The high fidelity orbit archives used for this purpose were supplied by the Electro-Optics Technology Branch of the Naval Research Laboratory (NRL Code 8123) under the direction of Dr. G. Charmaine Gilbreath, with the assistance of Mark Davis of ATSC. In virtually all cases, the good GNP-1 and GNP-2 normal

points appear as identical. Occasionally, GNP-1 and GNP-2 normal points disagree at a different full-rate measurement chosen as the basis for the normal point bin.

As GNP-2 was designed to alleviate manual editing of noisy GPS data, a survey of all available GPS-35 passes between June 1, 1998 and July 31, 1998 were compared with NRL-supplied IGS orbits. During this span, no outliers were detected and GNP-2 provided 3 fewer normal points than GNP-1. Detailed analysis of the normal point differences revealed that GNP-2 failed to form 5 single-point normal points, but gained two normal points having 22 quality full rate data (comprising a net gain of 14 compressed full-rate observations that the total normal point count does not reflect). These differences occur because GNP-1 cannot always reliably span a trend function across very large data outages (approaching one hour), so GNP-2 subdivides the pass into segments when data outages exceed 22 minutes. Some of these sub-divided pass segments have fewer than the minimum number of observations required to perform trend analysis, which suppresses the formation of normal points in these sparse arcs.

Normal points for sixteen passes of GFZ-1 spanning May 13, 1998 to May 22, 1998 were also reconstructed from archived full-rate data submitted by five stations. These were compared with the GNP-1 normal points, full rate data, and an NRL-supplied orbit. Although the orbit is not as good (making it difficult to clearly categorize acceptable and unacceptable normal points), the 446 normal points generated were nearly identical.

18. Removal of Outliers

Rigorous validation of autonomous data screening was conducted on several hundred SLR passes using predicted IRV orbits of various (usually poor) quality. Some 80 worse-case passes were especially scrutinized during periods where the GNP-1 had been known to produce erroneous normal points and where the full-rate data were available at the CDDIS archive. Using identical data, GNP-2 suppressed all the bad normal points generated by GNP-1 (see Table 2, Figure 1).

The four targets in Table 2 produced the greatest number of bad normal points for the station under analysis (Moblas 6, 7110). Except for Fizeau, which is the noisiest of the four satellites presented, the GNP-2 process produced more quality normal points than GNP-1 and generated no outliers. In a few cases where GNP-2 failed to make a quality normal point (compared to GNP-1), these points resided in the sparse, sub-divided passes discussed earlier.

Although beyond the scope of this paper, independent validation campaigns have been conducted. Detailed analyses on at least 48 passes by Brion Conklin of ATSC were instrumental in quality assessment of GNP-2, and expanded analyses continue at the time of this writing. Julie Horvath of ATSC has been operating experimental versions of GNP-2 for several months as part of the manual qualification of GPS tracking. This work has provided the many case studies that rendered improvements to the GNP process.

19. Recommendations for the Future

The GNP-2 analyses show no statistically significant range difference between the GNP-2 and GNP-1 normal points estimates, and the adopted tuning constants suggested by Holland and Welsch (1977) provide a high level of asymptotic efficiency with a standard normal distribution. More recent discussions in the literature (Sinclair, 1992; Sinclair, 1995b) have advocated accounting for small differences between the mode and the mean of the return distribution. This is accomplished with a highly trimmed Gaussian distribution (or rather its “peak-finding” approximation). It is possible that other robust estimators might adequately compensate for such distributional skewness, provided the tracking density is sufficient.

In both GNP-1 and GNP-2, one occasionally sees a pass where the modified short-arc DC is unable to converge satisfactorily, so that the remaining signal must be removed solely with the bias function. Improving the IRV models and abandoning the finite-difference partial derivative approximation would likely reduce the number cases in which this occurs. Bias analysis in RTN space is likely to be especially advantageous and may be eventually implemented in future versions of the normal point processor.

20. Summary

The GNP-2 normal point processor is a fully operational software package that has undergone various levels of benchmarking, and its release is expected into the public domain in the near term pending final reviews. This paper presents a cursory theoretical foundation with supporting references for potential users, and cites specific operational changes from its predecessor, GNP-1. Some test cases are presented which are part of a complete authentication effort

underway by several interested individuals and agencies. The GNP-2 process represents design trade-offs made in the face of certain constraints both mandatory and artificially imposed, but nevertheless presents a measurable improvement to the existing NASA software.

E. Acknowledgments

The author gratefully acknowledges the support of NASA GSFC and the technical staff at AlliedSignal Technical Services Corporation Earth Sciences Division, most notably Brion Conklin, Julie Horvath, Van Husson, and Scott Wetzel. Special appreciation is extended to Mark Davis of ATSC for his assistance with data visualization, and to NRL Code 8123 and Dr. Charmaine Gilbreath for the use of reference trajectories.

F. Bibliography

Andrews, D.F., P.J. Bickel, F.R. Hampel, P.J. Huber, W.H. Rogers, J.W. Tukey; "Robust Estimates of Location: Survey and Advances." (1972), Princeton University Press., Princeton, NJ, USA.

Appleby, G.M., A.T. Sinclair; "Formation of On-Site Normal Points", Proceedings of the 8th International Workshop on Laser Ranging Instrumentation, Annapolis, Maryland, USA, 1992, pp. 9.19-9.25.

Coleman, D., P. Holland, N. Kaden, V. Klema, S.C. Peters; "A System of Subroutines for Iteratively Reweighted Least Squares Computations", ACM Transactions on Mathematical Software, Vol. 6, No. 3, Sep. 1980, pp. 327-336.

Conklin, B., M. Davis, D. Edge, V. Husson, U.K. Rao, G. Su; "NSLR PC Software Packages for Normal Point and Acquisition Generation", Proceedings of the 9th International Workshop on Laser Ranging Instrumentation, Canberra, Australia, November 7-11, 1994, pp. 1090-1095

Davis, G.W., J.C. Ries, B.D. Tapley; "The Accuracy Assessment of Precise Orbits Computed from Doppler Tracking Data", The Journal of the Astronautical Sciences, Vol. 45, No. 4, Oct.-Dec. 1997, pp. 451-469.

Fair, R.C.; "On the Robust Estimation of Econometric Models", Ann. Econ. Social Measurement (1974), 3, pp. 667-678.

Golub, G.H., C.F. Van Horn, *Matrix Computations* 2nd ed., (1989), John Hopkins University Press, Baltimore, MD, USA.

Hampel, F.R., E.M. Ronchetti, P.J. Rousseeuw, W.A. Stahel, *Robust Statistics - The Approach Based on Influence Functions*, 1985, John Wiley & Sons.

Holland, P.W., R.E. Welsch; "Robust Regression Using Iteratively Reweighted Least-Squares", 1977, Communications in Statistics, A6, pp. 813-827.

Huber, P.J.; *Robust Statistical Procedures (2nd ed.)*, 1996, Regional Conference Series in Applied Mathematics No. 68, Society for Industrial and Applied Mathematics (SIAM), Philadelphia, PA.

Huber, P.J.; *Robust Statistics*, 1981, John Wiley & Sons.

Jefferys, W.H., M.J. Fitzpatrick, B.E. McArthur; "GaussFit — A System for Least Squares and Robust Estimation" (1988), Celestial Mechanics 41, pp. 39-49.

Jefferys, W.H.; "Robust Estimation When More than One Variable Per Equation of Condition Has Error" (1990), Biometrika, 77, 3, pp. 597-607.

Jefferys, W.H., J.G. Ries; "Bayesian Analysis of Lunar Laser Ranging Data", Proceedings of the Second Conference on Statistical Challenges in Modern Astronomy, Penn State University June, 1996, pp. 49-65.

Paunonen, M.; "Adaptive Median Filtering for Preprocessing of Time Series Measurements", Proceedings of the 8th International Workshop on Laser Ranging Instrumentation, Annapolis, Maryland, USA, 1992, pp. 2.44—2.50.

Press, W.H., S.A. Teukolsky, W.T. Vetterling, B.P. Flannery; *Numerical Recipes in FORTRAN - The Art of Scientific Computing*, 2nd Ed., 1992, Cambridge University Press.

Rey, W.J.J.; *Introduction to Robust and Quasi-Robust Statistical Methods*, Springer-Verlag, 1983.

Ricklefs, R., p. Shelus; "Poisson Filtering of Laser Ranging Data", Proceedings of the 8th International Workshop on Laser Ranging Instrumentation, Annapolis, Maryland, USA, 1992, pp. 9.26—9.32.

Sinclair, A.T.; “SLR Data Screening; Location of Peak of Data Distribution”, Proceedings of the 8th International Workshop on Laser Ranging Instrumentation, Annapolis, Maryland, USA, 1992, pp. 2.34-2.43.

Sinclair, A.T.; “An Assessment of the IRV Model for Very Low and Very High Satellites”, Proceedings of the 9th International Workshop on Laser Ranging Instrumentation, Canberra, Australia, November 7-11, 1994, pp. 381-387.

Sinclair, A.T. (ed.); Proceedings of the Annual EUROLAS Meeting: Satellite signature effects on SLR / Properties of avalanche photo diode detectors for SLR, Munich, March 1995a.

Sinclair, A.T.; “Data Screening and peak location”, Proceedings of the Annual EUROLAS Meeting: Satellite signature effects on SLR / Properties of avalanche photo diode detectors for SLR, Munich, March 1995b.

Sinclair, A.T.; “Data Screening and Normal Point Formation: A Restatement of the Herstmonceaux Normal Point Recommendation”, July 18, 1997 via URL http://cddisa.gsfc.nasa.gov/cstg/npt_algo.html

Detong, Tan, Zhang Zhongping, Xu Huanguan, Jia Peizhang; “Application of the Robust Estimate in SLR Data Preprocessing”, Proceedings of the 8th International Workshop on Laser Ranging Instrumentation, Annapolis, Maryland, USA, 1992, pp. 9.58–9.65.

Vallado, D.; *Fundamentals of Astrodynamics and Applications*, 1997, McGraw-Hill.

Wadsworth, H. M., Jr. (ed.), *Handbook of Statistical Methods for Engineers and Scientists*, 1989, McGraw-Hill

Watkins, D.S.; *Introduction to Matrix Computations*, 1991, John Wiley & Sons.

G. Figures, Tables, and Illustrations

Satellite	Normal Point Bin (sec)	Isolation Window (sec)
GFZ-1	5	60
ZEIA	5	60
ERS 1/2	15	60
FIZEAU	15	90
WESTPAC	15	90
STARLETTE	30	90
AJISAI	30	90
STELLA	30	90
GFO-1	30	90
TOPEX	15	240
LAGEOS-1/2	120	240
ETALON 1/2	300	600
GPS 35/36	300	600
GLONASS	300	600

Table 1. Isolation Intervals for Leverage Filtering

	GNP-1	GNP-2
STARLETTE	175 / 9	179 / 0
LAGEOS-1	578 / 16	585 / 0
LAGEOS-2	313 / 13	315 / 0
FIZEAU	293 / 18	290 / 0
GPS-35	254 / 0	251 / 0
GFZ-1	446/??	446/??

Table 2. GNP-2 vs. GNP-1 Benchmarked Normal Points (Acceptable / Unacceptable)

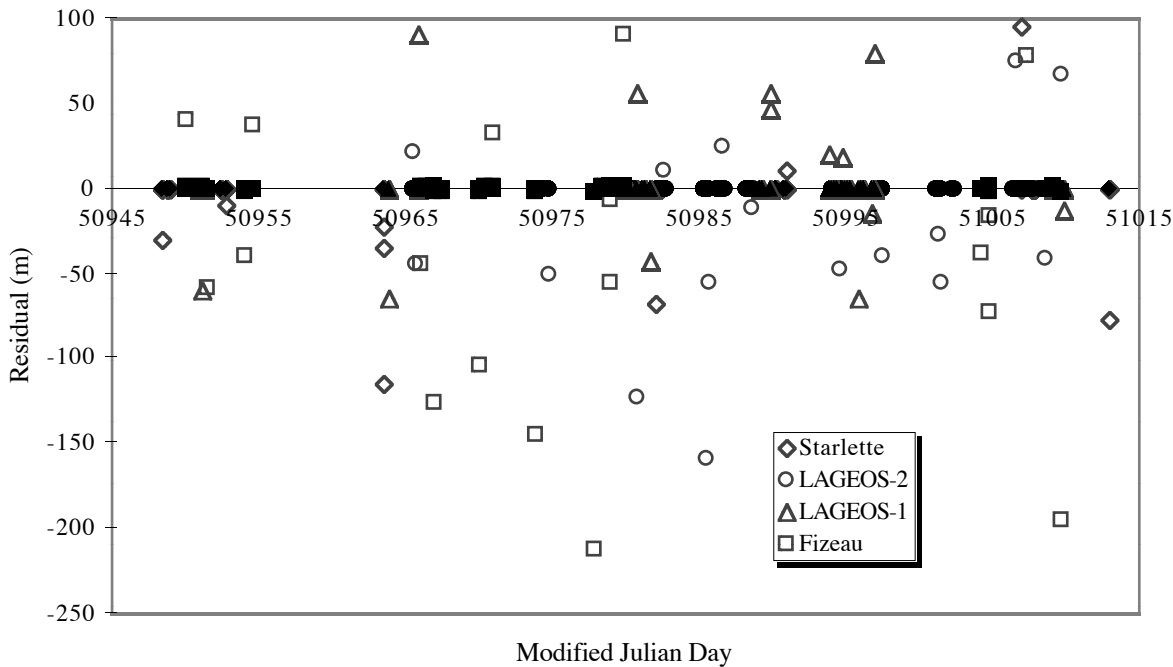


Figure 1. GNP-2 vs. GNP-1 Normal Point Residuals for Problem Passes (Station 7110)
(Dark Symbols indicate GNP-2 results using identical data)

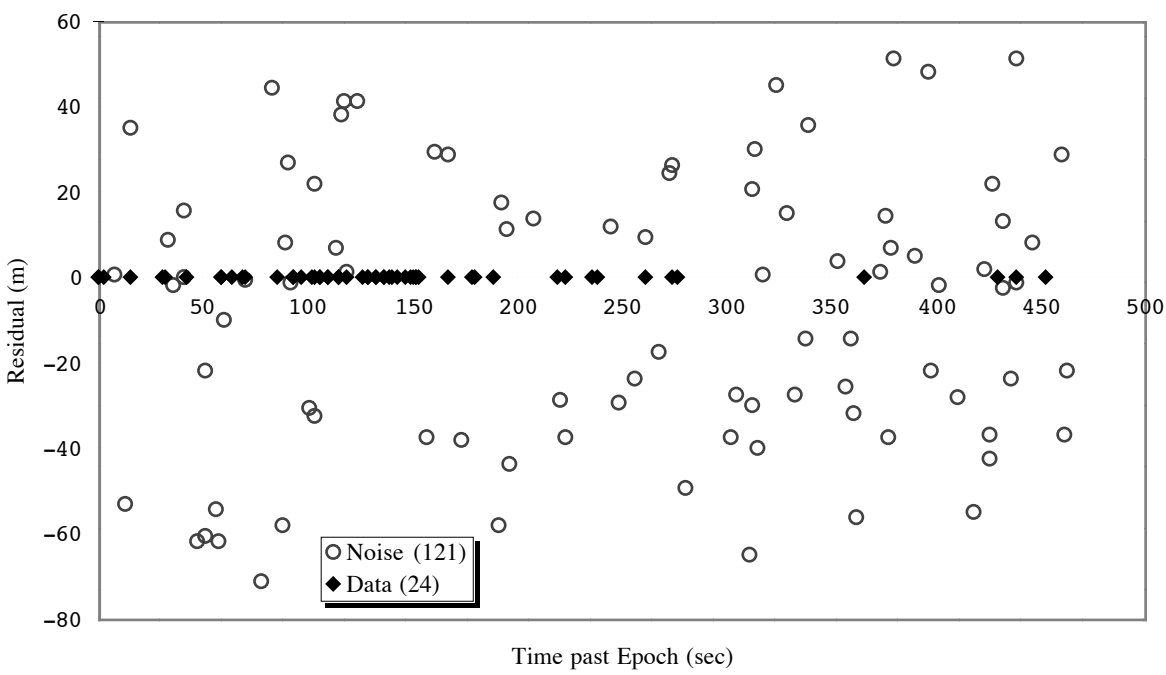


Figure 2. Median Pre-filter Discriminating Data from Noise (LAGEOS-2, Station 7110, 05/17/1998 19:31 UTC)

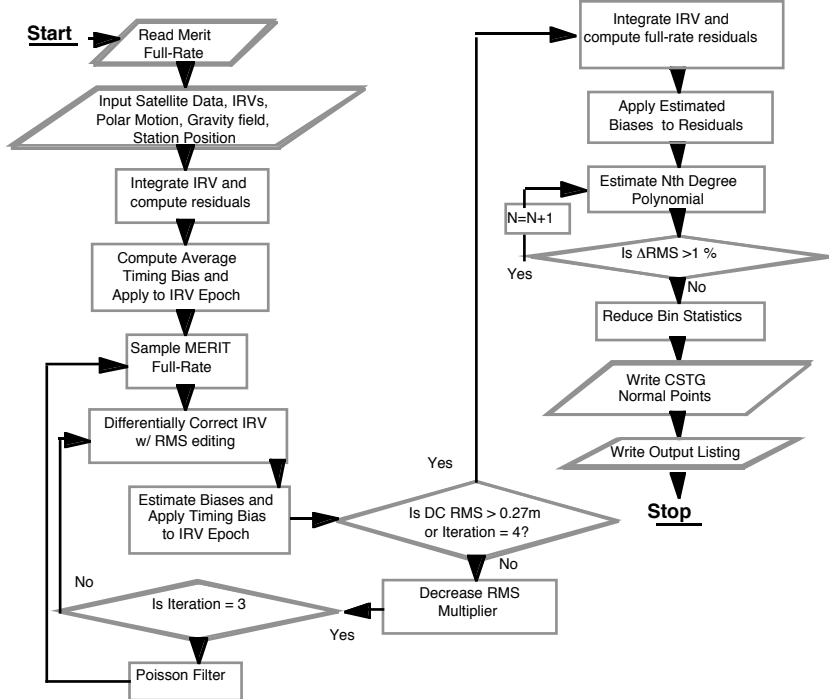


Figure 3. GNP-1 Process Flow (based on Conkin et al., 1994)

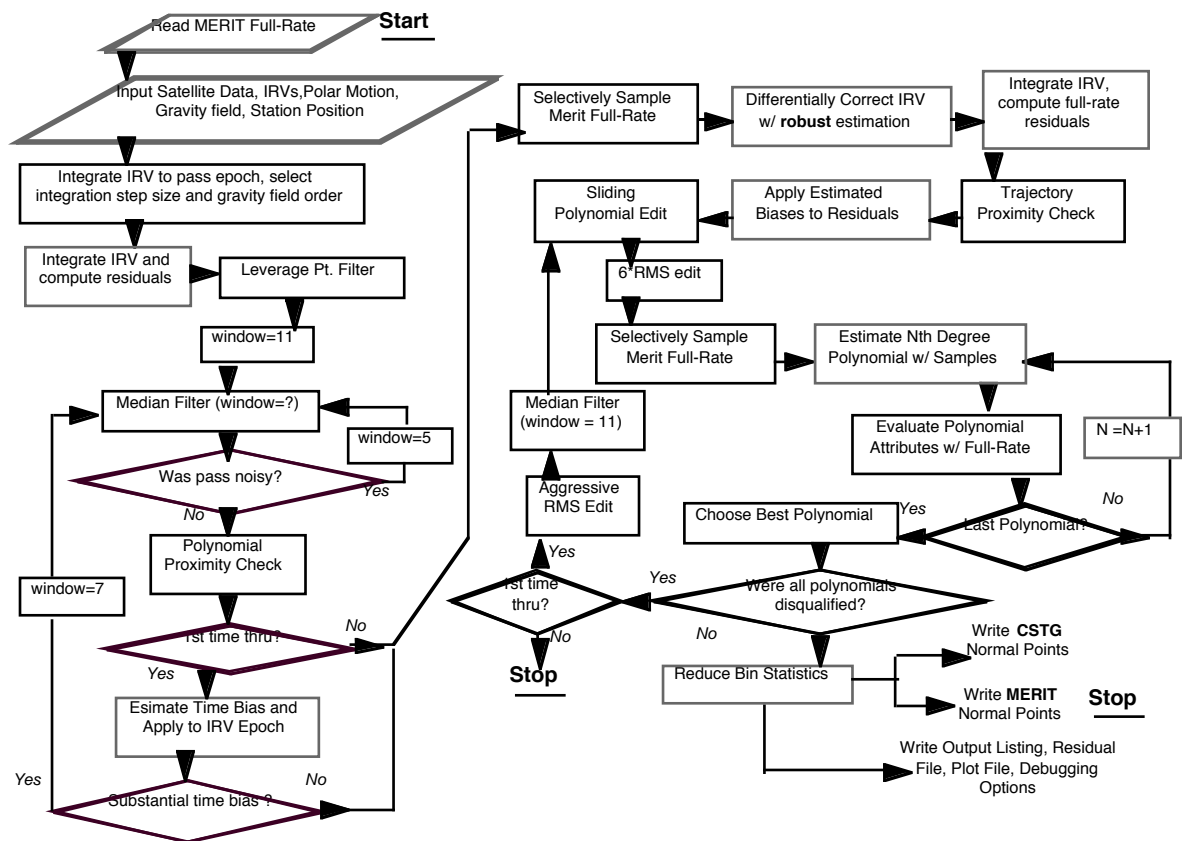


Figure 4. GNP-2 Process Flow